Bioinspired Adaptive Spiking Neural Network to Control NAO Robot in a Pavlovian Conditioning Task.

Alberto Antonietti[1], Claudia Casellato[2], Egidio D'Angelo[2,3] and Alessandra Pedrocchi[1]

Abstract— The cerebellum has a central role in fine motor control and in various neural processes, as in associative paradigms. In this work, a bioinspired adaptive model, developed by means of a spiking neural network made of thousands of artificial neurons, has been leveraged to control a humanoid NAO robot in real-time.

The learning properties of the system have been challenged in a classic cerebellum-driven paradigm, the Pavlovian timing association between two provided stimuli, here implemented as a laser-avoidance task. The neurophysiological principles used to develop the model, succeeded in driving an adaptive motor control protocol with acquisition and extinction phases.

The spiking neural network model showed learning behaviors similar to the ones experimentally measured with human subjects in the same conditioning task. The model processed in real-time external inputs, encoded as spikes, and the generated spiking activity of its output neurons was decoded, in order to trigger the proper response with a correct timing. Three long-term plasticity rules have been embedded for different connections and with different time-scales. The plasticities shaped the firing activity of the output layer neurons of the network.

In the Pavlovian protocol, the neurorobot successfully learned the correct timing association, generating appropriate responses. Therefore, the spiking cerebellar model was able to reproduce in the robotic platform how biological systems acquire and extinguish associative responses, dealing with noise and uncertainties of a real-world environment.

I. INTRODUCTION

The human nervous system is constituted by an ordered network of more than 10^{11} of neurons, specialized cells for information processing and transmission, connected by $10^{14} \sim 10^{15}$ synapses, where information is transferred from one neuron to the next one by means of electric or chemical signals (e.g. neurotransmitters). In general, neurons can be divided into two classes: excitatory and inhibitory, but there are many different types of neurons, each one with different morphologies, electrophysiological properties, dynamics and

[1]A. Antonietti and A. Pedrocchi are with the Neuroengineering and Medical Robotics Laboratory, Department of Electronics, Information and Bioengineering, Politecnico di Milano, Piazza L. da Vinci 32, Milano, Italy `alberto.antonietti@polimi.it`

[2]C. Casellato and E. D'Angelo are with the Department of Brain and Behavioral Sciences, University of Pavia, Via Forlanini 6, Pavia, Italy

[3] E. D'Angelo is with the Brain Connectivity Center, IRCCS Istituto Neurologico Nazionale C. Mondino, Via Mondino 2, Pavia, Italy

functions [1]. Roughly a half of the brain neurons constitute the cerebellum, an important organ for fine motor control. It receives data from multiple sensory channels (e.g., vestibular and proprioceptive), together with motor impulses, and modulates the activity of nuclear neurons, projecting towards cerebral cortex and spinal cord.

The function of the cerebellum was investigated for centuries and there are clear indications that the cerebellum central role concerns motor and associative learning tasks [2]. It is now accepted that the cerebellum is not only crucial for motor coordination, but is also involved in a range of non-motor functions and cognitive processes such as visual-shape discrimination, noun-verb association, attention and working memory [3].

A good paradigm for stressing the cerebellar role, which is investigated in this work, is the Pavlovian conditioning, e.g. the eyeblink conditioning [4], [5]. The eyeblink conditioning is an associative task where the subject has to learn the temporal association between a first stimulus, e.g. an auditory cue, called Conditioned Stimulus (CS), and a second stimulus, e.g. an air-puff directed toward the subject cornea, called Unconditioned Stimulus (US). The US is provided after a steady time-interval, called Inter-Stimulus Interval (ISI), which can range between 200 ms to more than 1000 ms [6], [7]. After few tens of trials, where the two stimuli are provided, the subject is able to implicitly learn the timing association between the CS and the US. As a result, the subject starts generating a Conditioned Response (CR), which is an eyelid closure anticipating the US, thus reducing the harmfulness of the air-puff. In this work, we have used a humanoid robot to reproduce the eyeblink conditioning protocol as a laser-avoidance task. The humanoid robot has to learn the timing association between two different stimuli (i.e. a tone (CS) and a laser beam (US)) and to react protecting himself (CR) moving a shield attached to its right arm, anticipating the laser beam.

Recently [8], [9], we have developed a bioinspired cerebellar model, using a Spiking Neural Network (SNN), and we have tested its learning performances with simulations of the eyeblink conditioning paradigm. The SNN model proved to be able to learn the timing association in few tens of trials, as in human beings, and it has been validated against experimental datasets even in altered conditions [10].

In this work, we have embedded the SNN controller into a humanoid robot, with the aim to reproduce the Pavlovian conditioning task in a real-world system and in noisy conditions. As a result, we have verified that the proposed cerebellar-inspired SNN was able to control in real-time
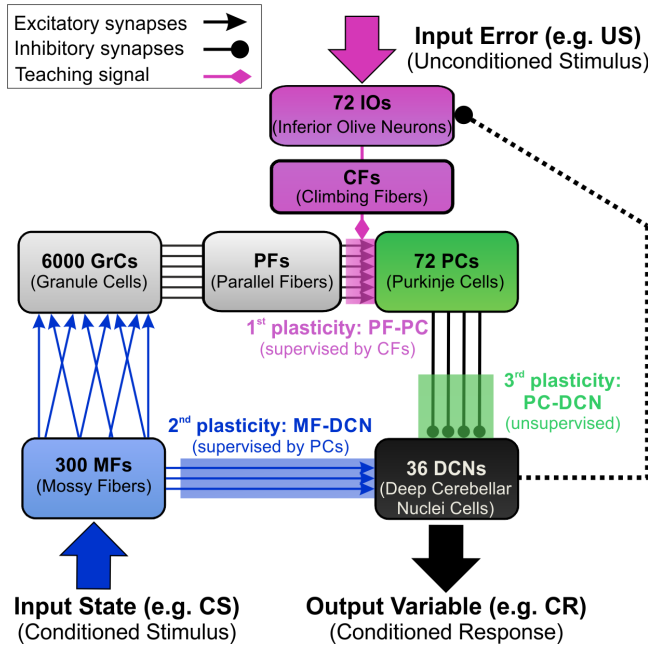
Fig. 1. **Cerebellar SNN.** The computational model applied for creating the cerebellar SNN embedded into the controller of NAO Robot. Each block represents a neural population, with the relative inputs and outputs. The excitatory, inhibitory and teaching connections are depicted. The shaded areas represent the three plasticity sites: in magenta the PF-PC synapses, in blue the MF-DCN synapses, and in green the PC-DCN synapses. Adapted from [11].

a humanoid robot, triggering CRs with the correct timing during a Pavlovian associative task, dealing with the noise introduced by non-ideal experimental conditions.

II. MATERIALS AND METHODS

A. Cerebellar Controller

The cerebellar SNN architecture was built taking inspiration from physiological studies of the cerebellum, in a tight collaboration with neuroscientists. The SNN (Fig. 1) was composed of 6480 Leaky Integrate&Fire neurons replicating the cerebellar microcircuit: 300 Mossy Fibers (MFs), the first input of the cerebellar network, encoding the state of the system; 6000 Granular Cells (GrCs), generating a sparse representation of the state input; 72 Inferior Olive neurons (IOs), the second cerebellar input, encoding the current "error" of the system or a more general attentive signal; 72 Purkinje Cells (PCs), the integrators of the sparse state-information coming from the GrCs through the Parallel Fibers (PFs) with the error-information coming from the IOs through the Climbing Fibers (CFs); 36 Deep Cerebellar Nuclei neurons (DCNs), which are the only output of the cerebellar microcomplex, thus producing the cerebellar output variable, i.e. triggering the motor response generated by the cerebellum.

MFs send projections to the GrCs, and each GrC received inputs from four MFs, 24000 excitatory synapses overall. The PFs connected each PC with ∼4800 GrCs, for a total of 345 444 synapses. The 72 CFs connected IOs and PCs with one to one teaching connections. DCN received a double input,

an excitatory one from MFs (10800 excitatory synapses) and an inhibitory one, from PCs (each DCN was inhibited by 2 PCs, for 72 overall synapses). We implemented an external DCN-IO inhibitory connection (dashed connection in Fig. 1), which halved the IO firing rate during the US following a CR [12].

The SNN model was equipped with three plasticity sites, at cortical (PF-PC) and nuclear (MF-DCN and PC-DCN) levels. The synaptic connections in each site followed three different learning rules, which strengthen or weaken these connections by long term modifications: Long Term Potentiation (LTP) and Long Term Depression (LTD). LTP and LTD mechanisms were modeled as modifications on the synaptic conductances as described in detail in [11], [9]. In general, the three mechanisms were based on different kinds of Spike-Timing-Dependent Plasticity (STDP), but each one was tailored to the specific experimentally-measured mechanism. The first plasticity (PF-PC) modulates the activity of PCs, increasing or decreasing the synaptic strength of the connections under the supervision of the IOs activity. The second plasticity (MF-DCN) is also a supervised learning rule, in this case, the PCs activity is the modulator signal that influences the synaptic weights. The third plasticity (PC-DCN) is an unsupervised standard STDP, where the weight modifications are driven uniquely by the timing of the pre-synaptic (PC) and post-synaptic (DCN) neurons.

To perform the simulations in real-time, we leveraged the EDLUT simulator [13], an open source simulator of SNN that provided a reduction of the computational loads, speeding up the network simulation by means of look-up-tables. In fact, with a standard simulator (e.g. NEURON [14], NEST [15], [16], or Brian [17]) the program has to solve one or more differential equations for each neuron and cannot guarantee the real-time performances that are required in interfacing a real robotic platform.

B. Robotic Setup and Testing Paradigm

The robot used to carry out the test was a NAO humanoid robot (H21 - V3.2, NAOQi 1.14.5, SoftBank Robotics, previously Aldebaran Robotics, France). NAO is characterized by 21 Degrees of Freedom (DoFs), actuated with brushed motors with rotation encoders. Each DoF can be commanded in position, setting a desired target angle, or in velocity, setting the motor velocity as direction and percentage of the maximum velocity. For the protocols, the movements involved the left arm of the robot. We thus controlled NAOs shoulder pitch, shoulder roll, and elbow roll. The cerebellar model ran on a laptop PC (Intel Quad-Core i7-4712MQ CPU @2.30 GHz with 16 GB of RAM with Windows 10 Pro N 64 bit), communicating with NAO via wired (Ethernet) connection. It is possible to communicate with NAO also through a wireless (Wi-Fi) connection, but it suffered from a lower connection stability and higher latencies.

The Pavlovian paradigm was designed to mimic human learning observed in neurophysiological studies, embedding the cerebellar SNN in the robot controller, customizing the input and output to the specific task.

The Pavlovian task (Fig. 2.A) consisted of 100 trials: 80 trials of acquisition and 20 trials of extinction. As a matter of fact, the protocol design foresaw a realistic time-lapse inspired by the time-lapse of human learning in eyeblink conditioning, thus we challenged the SNN with a realistic test-bench.

The acquisition phase, where CS-US pairs were presented, consisted of 80 trials. For each trial, the CS was generated as a random spike pattern on the 300 MFs at 50 Hz. The US was produced as a random spike pattern on the IOs with a firing rate of 10 Hz lasting 100 ms. The US time onset was triggered ∼850 ms after the CS onset. However, the ISI was not strictly repeatable, but it was subjected to a certain noise, due to the lower and unstable refresh rate of the NAO robot (∼50 Hz).

With NAO robot, the Pavlovian protocol was implemented as a laser-avoidance task [18], [19], [12]. While standing in its initial position, NAO was able to record sounds from its microphones. To appreciate the task, the CS was a tone, emitted by the PC loudspeaker; whereas the US was the activation of a red laser beam, commanded via serial communication. Both the tone and the laser were controlled by an *ad-hoc* C++ program, which managed also the SNN simulation. The tone was detected when the volume of the audio-track recorded by NAO microphones suddenly incremented with respect to the baseline low-amplitude environmental noise. The tone detection triggered the CS onset, carried by MF spikes in the cerebellar SNN. The US onset (the laser beam) was not detected by means of the NAO cameras, but it was triggered by the C++ program 850 ms after the generation of the tone. The US triggered IOs spikes, then carried by the CFs (Fig. 2.B). During the extinction phase, the laser pointer was not activated and hence the US signal was no longer elicited. The firing rate of DCNs was decoded into an analog variable (Output variable) with a frequency-based approach. When a DCN spike occurred, the output variable was increased, otherwise, it was decreased with an exponential decay. In order to avoid a jerky behavior of the output, the variable is filtered by means of a mobile average with a 50 ms window. A CR was detected when the filtered output variable overcome a fixed threshold, set to 100, before the US onset. Since the eyeblink conditioning is a pure timing association, the identified CR triggered a pre-programmed movement of NAO right arm, which protected the robot body from the laser beam.

C. Data Analysis

The 100 trials of the protocol were divided into blocks of 10 trials each. For each block, the number of CRs generated in the block was computed, and reported as a percentage of the maximum number of potential CRs (i.e. 10 CRs per block). Another important measure regards the anticipation (latency) of the CR, i.e. the time difference between the DCN activity causing a CR and the US onset.

15 tests (of 100 trials each) were carried out, in order to verify the robustness and the repeatability of the learning protocol, because the robotic platform introduced some vari-
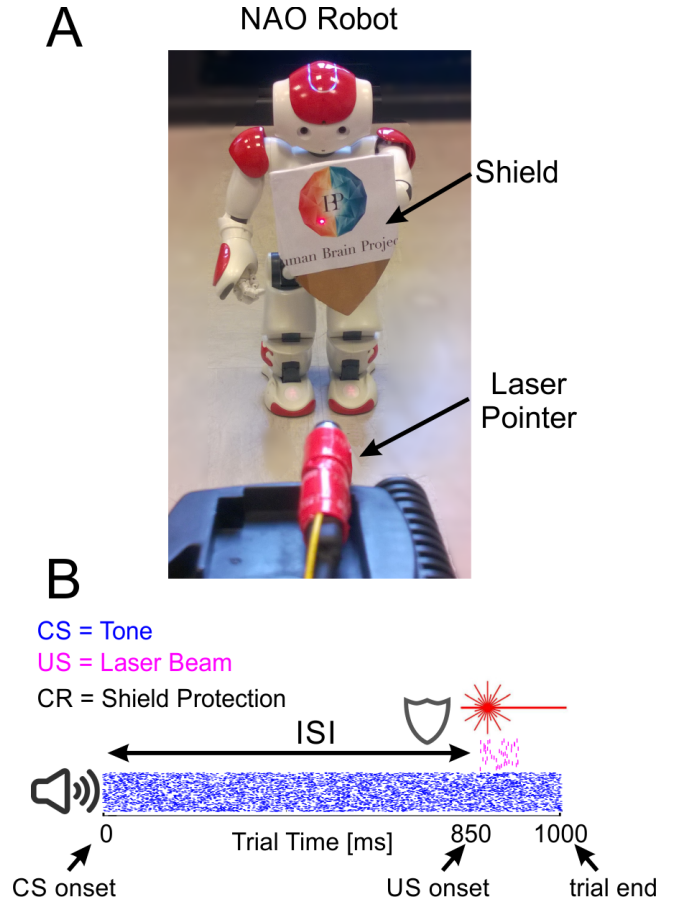

Fig. 2. **Robotic set-up and input/output signals of the protocol.** (A) and (B) show the Pavlovian task reproduced into the robotic platform as a laser-avoidance task. NAO robot needed to protect himself with the provided shield from the laser beam (US), which was activated ∼850 ms after the CS.

ability between one test and another. Since CR percentages were discrete variables, medians and interquartile intervals were reported, while means and standard deviations of the latency have been computed, for blocks where at least one CR was generated.

The spiking activity of the neurons was recorded for the whole protocol, and it was reported with raster-plots for three salient trials: the 1st trial of the acquisition, the 80th trial of acquisition, and the 100th trial (end of the extinction phase). In these three trials, the firing rates of the relevant neural population were reported, in order to show the firing activity evolution along the trials.

III. RESULTS

The 3-plasticity SNN, previously used uniquely on simulations of the EBCC protocol, here has been embedded with a humanoid robot. In order to test the learning skills of this neurorobot, we have designed a human-like sensorimotor task, addressing the timing associative capabilities of the brain-inspired SNN.

Acquisition and extinction were comparable to the one obtained with the simulated eyeblink conditioning protocol [9], in spite of the different ISIs between the two protocols

(850 ms *versus* 400 ms). In the late acquisition (blocks 6-8), a mean CR occurrence around 80% was achieved, similar to the CR percentage acquired by human subjects in neurophysiological experiments [20] (Fig. 3.A). Since we have tested the network in a robot interacting in the real-world, there were uncertainties on the ISI, which was not strictly fixed, as in the simulations. Indeed, the average ISI, considering all the 15 tests carried out, was equal to 850 ± 30 ms. It is possible to notice a certain variability in the individual behavior (CRs) of the 15 tests (each row of Fig. 3.B). However, the average behavior was consistent. Indeed, the interquartile intervals were always equal to zero except for block 7 and block 9, where the interquartile intervals were equal to 10% each. In these two blocks the variability was slightly higher because the CR% were oscillating between 80% and 90% for block 7 and returning toward 0% for block 9, the first block of the extinction phase.

Considering the timing of the CRs, it is possible to observe a slight evolution of the latencies along the acquisition trials (Fig. 3.C). Indeed, the latencies at the early acquisition (blocks 1 and 2) are greater than in the following blocks, where the CRs were closer to US onset, stabilizing their average value to -344 ± 16 ms. Since in block 10 there were no CRs, the latency bar and its standard deviation are not present.

During the 1000 ms of CS, the firing rate of MFs was equal to 39 ± 6 Hz, while the IOs frequency was equal to 13 ± 8 Hz during the 100 ms of US. MF pattern and frequency was constant for the whole protocol, while the IO firing rate was inhibited to 6 Hz for the trials where an effective CR was detected. PC behavior was modulated by PF-PC LTP and LTD; in the first trial (Fig. 4.A), PCs were spontaneously firing at a mean frequency of 73 ± 4 Hz, steadily inhibiting DCNs. In the late acquisition (Fig. 4.B), their frequency was reduced to 67 ± 18 Hz, thus promoting DCN activity, which increased from a complete silent condition to a firing rate of 3 ± 5 Hz, producing CRs anticipating the US. In the extinction phase, the CS alone was presented. For the first trials, the network output still produced CRs, but soon the learning was reversed. A complete extinction was achieved thanks to an increased PCs firing rate (85 ± 3 Hz) and the consequent DCNs re-inhibition (Fig. 4.C).

IV. DISCUSSION

With these findings, we have demonstrated that it was possible to embed in a robotic control loop a distributed plasticity SNN, previously tested uniquely in simulations [9]. Leveraging a realistic SNN control in a real world environment is more challenging than computational simulations. In the eyeblink conditioning paradigm, the non-ideality introduced by a real robotic body is limited to the instability of the communication between the SNN and the robotic plant, that led to a variability of the ISI, and of possible defections of tone identification. In more advanced paradigms, the sources of non-ideality introduced by the real robot increase (e.g. joint motor inaccuracy, sensor errors, etc.) leading to a higher amount of variability and making
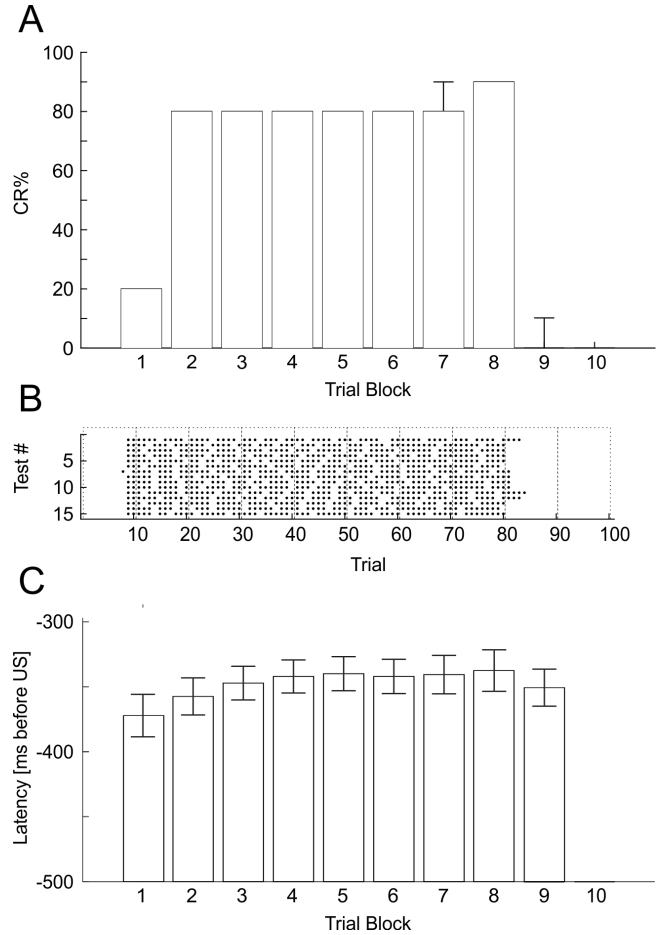

Fig. 3. **Pavlovian task with NAO robot: motor response generation.** (A) CRs percentage computed within each block of 10 trials. (B) shows the behaviors of the 15 tests, along the 100 trials of the protocol. The black dots represent the trials where a CR was generated. (C) CR latency evolution along the protocol. For each block, considering the whole 15 tests, means (bars) and standard deviations (whiskers) have been computed.

the task more challenging than simulations, even when those are artificially corrupted by noises.

Despite a computational load greater than other models already included in neurorobotic platforms [21], [18], [22], [12], the SNN was able to guarantee real-time performances, simulating the network activity with a standard laptop PC.

With respect to the cerebellar model used in [21], the present model was more than four times larger (6480 vs 1580 neurons) and endowed with distributed plasticities instead of a single plasticity mechanism (at PF-PC level). The SNN learned to adjust timing and gain of the motor responses by tuning its output, thus the system proved able to reproduce timing, prediction, and learning, which are the main abstract functions ascribed to the cerebellum [23], [24], [25], and allowed to investigate the spiking dynamics of the different network components.

The obtained performances, if compared to the ones presented in previous works, were enhanced. For instance, the number of trials needed to obtain stable acquisitions and extinctions was reduced tenfold, if compared to a smaller SNN with a single active plasticity [26]. This can be the
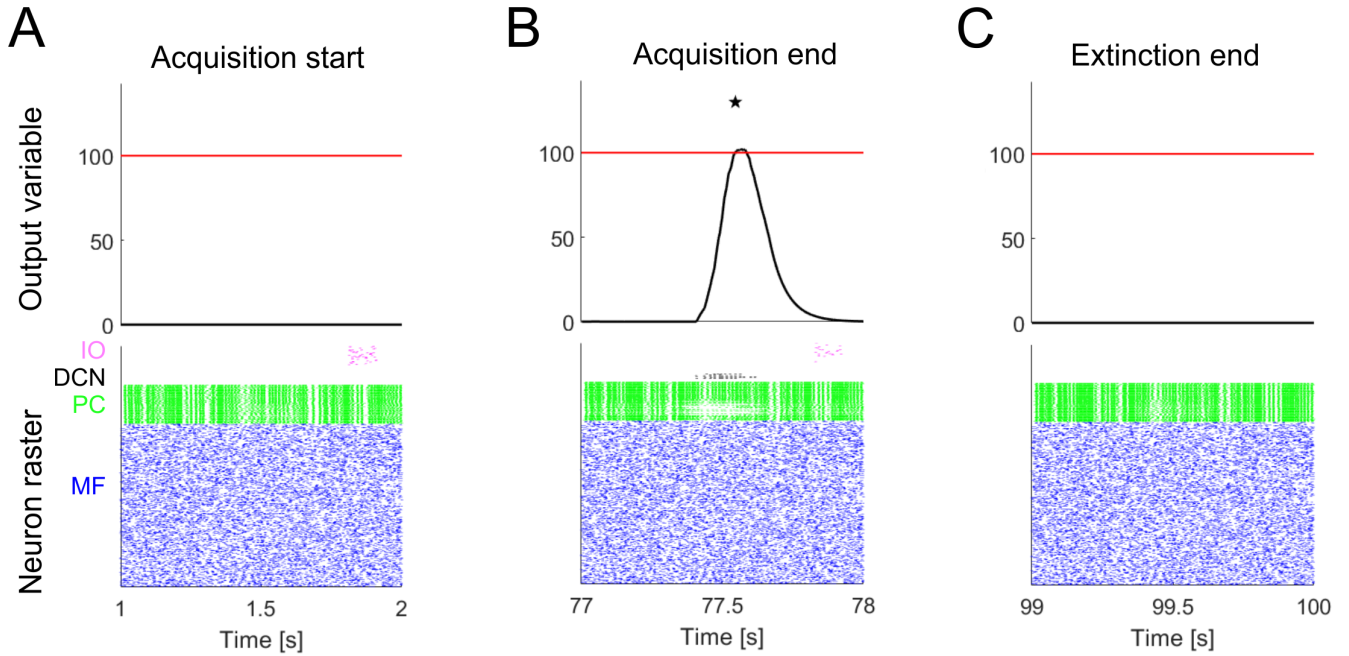
Fig. 4. **Neuron raster-plots of three salient trials of the Pavlovian associative protocol.** The three plots show the raster-plot of the SNN neurons (for clarity, we have excluded the GrCs), in three salient trials: the acquisition phase start, when the DCNs were silent; the acquisition end, when a stable CR generation was achieved, and the extinction end, where the DCNs returned to be silent. As showed in panel B, the weight modifications induced a time-specific depression at PF-PC synapses, thus selectively silencing PC activity and, as a consequence, increasing the DCN activity, which overcame the threshold (red line) just before the US onset. Hence, a CR was detected.

results of both the increase in the network size and the addition of nuclear plasticity mechanisms. By increasing the network size, we enhanced the circuit resolution, both at the input and at the output of the network. Indeed, with a larger number of neurons, we can encode and decode with a greater precision the input and the output signals, a concept similar to the number of bits of Analog-Digital Converters. In the eyeblink protocol, the input signal that triggers the MF activity is a binary input, hypothetically encodable with a single neuron. However, as recorded in neurophysiological experiments, it generates complex neural pattern at the level of MFs and GrCs, which encode not only the CS onset, but also the passage of time from the onset to the end of the trail. That is the reason why it is advantageous to have a higher number of neurons, because the complexity of the input patterns can be increased, leading to a better non-recurrence of a specific time step with the others. In this way, for each time step of the trial, there will be a unique combination of GrCs spikes, which can then provide a representation of the passage of the time that is necessary to associate the CS onset with the US onset.

With the addition of the nuclear plasticities, we expect also an improvement, but in particular, a learning acceleration on subsequent acquisition sequences, which should be faster when the SNN has multiple plasticity mechanisms. Additional tests foreseeing a two-session protocol could confirm this expectation.

The bottleneck of the refresh rate was represented by the interaction with NAO robot. The maximum possible refresh rate in this protocol, which used the NAO microphones, was equal to 50 Hz, 20 times lower than the update rate of the network (1 kHz). Also, the real-time communication with NAO was not guaranteed and this, together with the intrinsic noise of a device interacting with the real world, caused the not exact repeatability of the 15 tests. However, the standard deviations were limited and the general behaviors were clear and stable.

The firing rates of the different neural populations were comparable to the neurophysiological ranges measured experimentally [27], [28]: MFs 10-50 Hz, GrCs 5-15 Hz, IOs 1-2 Hz, PCs 50-100 Hz, DCNs 10-25 Hz. Moreover, their firing rates changed in a characteristic manner along the acquisition and extinction phases. These dynamic changes proved consistent with those revealed in experiments with ferrets [29].

As a future step, an articulated robotic platform as NAO can give us the possibility to design multi-dimensional control problems, going toward a greater realism also in terms of human-like controlled plants. Since it is our unique interface with the environment, having a realistic body model is as important as having a realistic brain model. NAO, with its 21 actuated DoFs and rich arrays of sensors (vision, auditory functions, touch sensors, gyroscopes, and accelerometers) can be potentially used to reproduce a large variety of behavioral tests, involving the cerebellum, but also other brain areas (visual and auditory cortex, hippocampus, etc.).

V. CONCLUSIONS

The robotic platform with its brain-inspired controller was able to reproduce the human behavior when dealing with

a cerebellum-driven task. The developed SNN had a topology that was a simplified model of the neurophysiological cerebellar network, including neural connectivity, plasticity mechanisms, and simplified neuron dynamics. The Pavlovian conditioning protocol tested the model capability to learn the temporal associations between two stimuli (an auditory cue and a visual cue) provided to the humanoid NAO robot.

In conclusion, the developed platform is a real neurorobot able to operate in a dynamic and noisy environment, dealing with a simple learning motor task. In the near future, it would be interesting to challenge the same SNN, here tested in a simple timing associative task, into multiple cerebellar-related paradigms. Possible suitable protocols that would be able to leverage in full the learning capabilities of the neuro-robot could be fine motor control adaptation (e.g. correcting an unexpected external perturbing force) or balance tasks. On a longer time-frame, the proposed biology-driven approach could be adopted to develop a generalized adaptive controller usable also in other robotic applications which have the requirements to adapt their actions in response to unexpected perturbations and in mutable conditions.

REFERENCES

[1] E. Kandel, J. Schwartz, and T. Jessell, *Principles of Neural Science, Fifth Edition*. Principles of Neural Science, McGraw-Hill Education, 2013.

[2] E. D'Angelo, A. Antonietti, S. Casali, C. Casellato, J. A. Garrido, N. R. Luque, L. Mapelli, S. Masoli, A. Pedrocchi, F. Prestori, M. F. Rizza, and E. Ros, "Modeling the Cerebellar Microcircuit: New Strategies for a Long-Standing Issue," *Frontiers in Cellular Neuroscience*, vol. 10, no. July, p. 176, 2016.

[3] M. Kawato and D. M. Wolpert, "Internal models for motor control," *Sensory Guidance of Movement*, vol. 218, pp. 291–307, 1998.

[4] G. T. Bartha and R. F. Thompson, "Cerebellum and conditioning," *The handbook of brain theory and neural . . .* , pp. 169–172, 1998.

[5] R. F. Thompson, "Neural mechanisms of classical conditioning in mammals," *Philosophical Transactions of the Royal Society of London. Series B: Biological Sciences*, vol. 329, pp. 161–170, 8 1990.

[6] D. H. Lindquist, R. W. Vogel, and J. E. Steinmetz, "Associative and non-associative blinking in classically conditioned adult rats," *Physiology & behavior*, vol. 96, pp. 399–411, 3 2009.

[7] R. W. Vogel, J. C. Amundson, D. H. Lindquist, and J. E. Steinmetz, "Eyeblink conditioning during an interstimulus interval switch in rabbits (Oryctolagus cuniculus) using picrotoxin to disrupt cerebellar cortical input to the interpositus nucleus.," *Behavioral neuroscience*, vol. 123, pp. 62–74, 2 2009.

[8] A. Antonietti, C. Casellato, E. D'Angelo, and A. Pedrocchi, "Model-driven analysis of eyeblink classical conditioning reveals the underlying structure of cerebellar plasticity and neuronal activity," *IEEE Transactions on Neural Networks and Learning Systems*, vol. PP, pp. 1–15, 9 2016.

[9] A. Antonietti, C. Casellato, J. A. Garrido, N. R. Luque, F. Naveros, E. Ros, E. DAngelo, A. Pedrocchi, E. D'Angelo, and A. Pedrocchi, "Spiking Neural Network With Distributed Plasticity Reproduces Cerebellar Learning in Eye Blink Conditioning Paradigms.," *IEEE Transactions on Biomedical Engineering*, vol. 63, pp. 210–9, 1 2016.

[10] A. Geminiani, C. Casellato, A. Antonietti, E. D'Angelo, and A. Pedrocchi, "A Multiple-Plasticity Spiking Neural Network Embedded in a Closed-Loop Control System to Model Cerebellar Pathologies.," *International journal of neural systems*, p. S0129065717500174, 1 2017.

[11] A. Antonietti, C. Casellato, J. A. Garrido, E. D'Angelo, and A. Pedrocchi, "Spiking cerebellar model with multiple plasticity sites reproduces eye blinking classical conditioning," in *2015 7th International IEEE/EMBS Conference on Neural Engineering (NER)*, vol. 2015-July, pp. 296–299, IEEE, 4 2015.

[12] I. Herreros and P. F. M. J. Verschure, "Nucleo-olivary inhibition balances the interaction between the reactive and adaptive layers in motor control," *Neural Networks*, vol. 47, pp. 64–71, 11 2013.

[13] E. Ros, R. R. Carrillo, E. M. Ortigosa, B. Barbour, and R. Agís, "Event-driven simulation scheme for spiking neural networks using lookup tables to characterize neuronal dynamics," *Neural computation*, vol. 18, pp. 2959–93, 12 2006.

[14] M. L. Hines and N. T. Carnevale, "Neuron: A Tool for Neuroscientists," *The Neuroscientist*, vol. 7, pp. 123–135, 4 2001.

[15] M.-O. Gewaltig and M. Diesmann, "NEST (NEural Simulation Tool)," 2007.

[16] H. E. Plesser, M. Diesmann, M.-O. Gewaltig, and A. Morrison, "NEST: the Neural Simulation Tool," in *Encyclopedia of Computational Neuroscience*, pp. 1849–1852, New York, NY: Springer New York, 2015.

[17] D. Goodman, "Brian: a simulator for spiking neural networks in Python," *Frontiers in Neuroinformatics*, vol. 2, no. November, p. 5, 2008.

[18] C. Hofstotter, M. Mintz, and P. F. M. J. Verschure, "The cerebellum in action: a simulation and robotics study," *European Journal of Neuroscience*, vol. 16, pp. 1361–1376, 10 2002.

[19] T. Yamazaki and J. Igarashi, "Realtime cerebellum: A large-scale spiking network model of the cerebellum that runs in realtime using a graphics processing unit," *Neural Networks*, vol. 47, pp. 103–111, 11 2013.

[20] V. Bracha, L. Zhao, K. B. Irwin, and J. R. Bloedel, "The human cerebellum and associative learning: dissociation between the acquisition, retention and extinction of conditioned eyeblinks," *Brain Research*, vol. 860, pp. 87–94, 3 2000.

[21] C. Casellato, A. Antonietti, J. A. Garrido, R. R. Carrillo, N. R. Luque, E. Ros, A. Pedrocchi, and E. D'Angelo, "Adaptive Robotic Control Driven by a Versatile Spiking Cerebellar Network," *PLoS ONE*, vol. 9, p. e112265, 11 2014.

[22] T. Yamazaki and S. Nagao, "A computational mechanism for unified gain and timing control in the cerebellum," *PloS one*, vol. 7, p. e33319, 1 2012.

[23] E. D'Angelo, S. Solinas, J. Mapelli, D. Gandolfi, L. Mapelli, and F. Prestori, "The cerebellar Golgi cell and spatiotemporal organization of granular layer activity," *Frontiers in Neural Circuits*, vol. 7, 2013.

[24] C. Miall and D. M. Wolpert, "Forward models for physiological motor control," *Neural networks*, vol. 9, no. 8, pp. 1265–1279, 1996.

[25] R. B. Ivry and J. V. Baldo, "Is the cerebellum involved in learning and cognition?," *Current opinion in neurobiology*, vol. 2, pp. 212–6, 4 1992.

[26] C. Casellato, A. Antonietti, J. A. Garrido, A. Pedrocchi, and E. D'Angelo, "Distributed cerebellar plasticity implements multiple-scale memory components of Vestibulo-Ocular Reflex in real-robots," in *Proceedings of the IEEE RAS and EMBS International Conference on Biomedical Robotics and Biomechatronics*, pp. 813–818, IEEE, 8 2014.

[27] J. F. Medina, K. S. Garcia, W. L. Nores, N. M. Taylor, and M. D. Mauk, "Timing mechanisms in the cerebellum: testing predictions of a large-scale computer simulation.," *The Journal of Neuroscience*, vol. 20, pp. 5516–25, 7 2000.

[28] R. Maex and E. D. Schutter, "Synchronization of Golgi and Granule Cell Firing in a Detailed Network Model of the Cerebellar Granule Cell Layer Synchronization of Golgi and Granule Cell Firing in a Detailed Network Model of the Cerebellar Granule Cell Layer," *Journal of Neurophysiology*, vol. 80, pp. 2521–2537, 2013.

[29] A. Rasmussen, D.-A. Jirenhed, D. Z. Wetmore, and G. Hesslow, "Changes in complex spike activity during classical conditioning," *Frontiers in neural circuits*, vol. 8, p. 90, 1 2014.